SCK • CEN

STUDIECENTRUM VOOR KERNENERGIE
CENTRE D'ÉTUDE DE L'ÉNERGIE NUCLÉAIRE

Constraint Assessment in PCCv and 1T C(T) Specimens using 3-D Finite Element Simulations

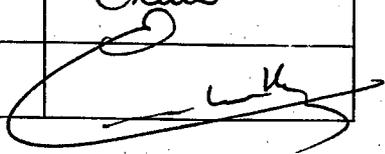Convention Electrabel-SCK•CEN

M. Scibetta

RMR
SCK•CEN, Mol, Belgium

DISTRIBUTION LIST

This document has been written and approved by:

		Date	Approval
Author:	M. Scibetta	28-11-00	MScibetta
Verified by:	E. Lucon	5/12/00	ELucon
Approved by:	E. van Walle	1-12-00	

Constraint Assessment in PCCv and 1T C(T) Specimens using 3-D Finite Element Simulations

Convention Electrabel-SCK•CEN

M. Scibetta

BLG-861

TABLE OF CONTENTS

ABSTRACT

The objective of this work is to compare the constraint of two standard geometries using three-dimensional finite element calculations. The selected geometries are the precracked Charpy V-notch, PCCv, and the one inch thick Compact Tension, 1T C(T), specimen statically loaded respectively in three point bending and in tension. In both cases, the crack length equals half of the specimen width.

It is found that the formulation proposed in the ASTM E1921-97 to calculate the J-integral for a C(T) specimen is accurate enough for its application. The maximum error on the reference temperature is 3 °C.

The constraint of PCCv and C(T) specimens at low load levels is close to the reference SSY plane strain solution. The constraint is even higher than the SSY solution just ahead of the crack tip. When the load increases, loss of constraint develops for the PCCv specimen geometry. Using a cleavage scaling model, it is found that this loss of constraint is responsible for reference temperatures about 10 °C lower as compared to the standard 1T C(T) specimen.

Another field of application is the correction of constraint for existing data set that contains few or any valid data.

KEYWORDS

Finite element calculations, three-dimension, PCCv, C(T), loss of constraint, fracture toughness

1 Introduction

Fracture toughness testing in the transition regime was recently standardised within the ASTM E1921-97 [1]. This standard proposes a normalised procedure to analyse the test results of standard specimens and to determine the reference temperature, T_0, for ferritic steels in the transition range.

The embrittlement of Reactor Pressure Vessel Steels (RPVS) could be usefully assessed through the shift of the reference temperature ΔT_0 instead of the current semi-empirical methodology. In practice, standard one inch thick Compact Tension, 1T C(T), specimens can be usefully replaced with smaller fracture toughness specimens, such as the precracked Charpy V-notch Specimen (PCCv). Indeed, irradiated RPVS are available in small quantities and PCCv specimens can be reconstituted from broken surveillance Charpy specimens [2].

The published literature shows that the PCCv specimen analysed using the ASTM E1921-97 standard generally shows a 10 °C lower reference temperature than the C(T) specimen. Compared with the inherent scatter in the transition, this difference is small. However, it has been observed on many materials [3]: JSPS [4, 5], 22NiMoCr37 [5], JRQ [5, 6], 73W [5], KFY5 [6] and JFL[6].

The reason for this difference can be:

- a non adequate formulation to derive the fracture toughness from the load displacement record,
- a different level of constraint in single edge notch bend SE(B) and C(T) geometries [4, 7, 8],
- a different level of constraint due to side-grooving,
- a different level of constraint due to the ratio W/B which is 1 for PCCv and 2 for C(T) and SE(B) [4],
- an inadequate size limit defined to avoid loss of constraint [4],
- a lower reference temperature corresponding to a lower test temperature, as PCCv specimens are generally tested at lower temperatures to increase the number of valid data.

The formulation and the level of constraint can be investigated using finite element simulations of the PCCv and 1T C(T) fracture toughness test. However, a simple 2-dimensional analysis of a PCCv specimen, assuming a plane strain behaviour, is not an adequate model to accurately describe the actual 3-dimensional geometry [9, 10].

The recommendations of ASTM E1921-97 to derive the fracture toughness from the load versus displacement record and to use a size limit to avoid loss of constraint are partly based on the work of Nevalainen and Dodds [10]. They performed a thorough 3-dimensional finite element analysis of the C(T) and SE(B) specimens. They provided:

- η-factors that are to be used to experimentally evaluate the fracture toughness,
- specimen size limits allowing a limited loss of constraint (10% overestimated fracture toughness),
- an effective thickness introduced for the statistical correction, which takes into account triaxiality changes along the crack front.

It is important to note that the current ASTM E1921-97 specimen size requirement is less severe than the specimen size requirement established by Nevalainen and Dodds in [10]:

$$b, B > \frac{MK^2}{E\sigma_{YS}}$$ (1)

with B the specimen thickness, b the ligament, K the fracture toughness, E the young modulus, σ_{YS} the yield stress and M a constant.

M=30 for ASTM E1921-97 and M=55 according to [10] for a strain hardening exponent n=0.1.

The application of equation (1) to a PCCv specimen with b=5 mm, E=205 GPa and σ_{YS}=500 MPa has for consequence that PCCv specimens that break between 96.5 for M=55 and 130 MPa√m for M=30 are subject to a significant loss of constraint. This loss of constraint is such that the fracture toughness might be overestimated by more than 10%. This overestimated fracture toughness might explain the lower reference temperature measured with PCCv specimens. Indeed, 10% higher median fracture toughness corresponds to a 6 °C lower reference temperature.

In order to develop a loss of constraint correction factor for small specimens and to gain confidence in the results presented in [10], a study was performed at SCK•CEN. This work was performed within Task 1.1.3 of the ELECTRABEL -SCK•CEN Convention 2000.

In a previous report [11], a finite element simulation of a fracture toughness test on a PCCv specimen was thoroughly investigated. It was found that the different formulations proposed in the ASTM E1921-97 to calculate the J-integral are sufficiently accurate for its application. The maximum error on the reference temperature is 3 °C.

In this report, the finite element calculation of a 1T C(T) specimen loaded up to 100 MPa√m is performed to obtain a reference condition. This reference condition is used to compare constraint levels in the two geometries.

2 FE model

To model actual material behaviour, the incremental theory of plasticity is used in combination with an isotropic strain-hardening model based on the Von Mises criterion with a uniaxial true stress versus true strain function described by a power law:

$$\frac{\sigma}{\sigma_{YS}} = \begin{cases} \dfrac{\varepsilon}{\varepsilon_{YS}} & \text{if } \sigma < \sigma_{YS} \\[2ex] \left(\dfrac{\varepsilon}{\varepsilon_{YS}}\right)^n & \text{if } \sigma \geq \sigma_{YS} \end{cases}$$ (2)

$$\text{with} \quad \varepsilon_{YS} = \sigma_{YS} / E$$ (3)

The actual true stress versus true strain behaviour of metallic materials can generally be fitted by a power law curve. Alternatively, the strain-hardening exponent can be obtained from the

following equation (4), which can easily be solved with a non-linear iterative solver. This expression was derived in [12] by solving the instability point and converting true stress to engineering stress.

$$\frac{\sigma_{TS}}{\sigma_{YS}} = \frac{\left(\dfrac{n}{\varepsilon_{YS}}\right)^n}{\exp(n)}$$

(4)

This study is limited to one material, representative of most unirradiated RPVS. It has a hardening exponents n=0.1, a Young modulus E=207 GPa, a Poisson ratio v=0.3 and a yield stress such that E/σ_{YS} =500.

As most of valid fracture toughness tests on PCCv and C(T) specimens do not show any ductile crack growth, the modelling of ductile crack growth by a complex node release technique is not necessary.

8-node isoparametric hexahedral elements without reduced Gauss integration are used.

Because of large geometry changes, the modified updated Lagrangian [13] procedure is used to account for large strains and displacements. To avoid large mesh deformation and overlapping at the crack tip, an initial blunted mesh is used. The initial crack tip radius is 10 μm. The dimension of the smallest element located at the crack tip is typically one third of the initial crack tip radius.

The specimen dimensions are for a 1T C(T): W=50 mm and B=25 mm. As ASTM E1921-97, states that a_0 shall be 0.5W±0.05W, a/W=0.5 is selected for the present study. To reduce computer time, only one fourth of the C(T) geometry was simulated (see Figure 1). Symmetry conditions were imposed to the planes defined by the equations y=0 and z=0. For the side-grooved geometry, the thickness reduction is 20%, the side-grooves angle 45° and the side-grooves radius 0.5 mm in accordance with ASTM E1921-97. The side-grooved mesh was obtained by modifying the non side-grooved mesh. The nodes for which $y<y_{sg}$ are translated in the z direction, where $2y_{sg}$ is the side-groove width given by:

$$y_{sg} = \tan(\alpha/2)\left(d + r\left(\frac{1}{\sin(\alpha/2)} - 1\right)\right)$$

(5)

where α is the side-groove angle, r the side-groove radius and d the side-groove depth.

For z=-12.5 the nodes are translated to reproduce the side-groove shape. For z≠0, the translation vector reduces linearly from z=-12.5 to z=0. The machined notches for precracking and for clip gauge attachment are not modelled, as this will not affect the results.
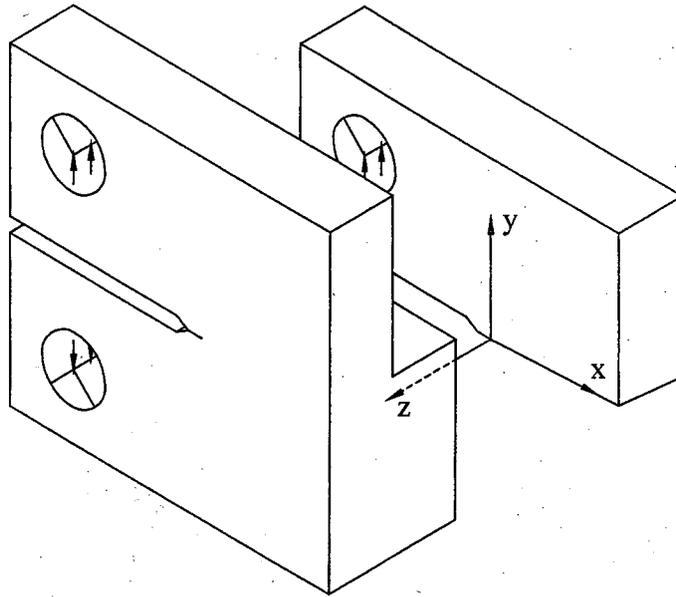
Figure 1 *C(T) specimen loaded in tension. Only one fourth of the geometry is simulated.*

Load application are contact conditions between the specimen and the loading pin. The introduction of these conditions in a finite element model is rather complex and introduces additional highly non-linear equations.

To simplify the problem, the contact is simulated by fixing the displacement in the $\bar{Y}$ direction on the nodes located on the centre of the hole. Elastic pentahedrons with the same Young modulus and Poisson ratio as the specimens are used to improve the load distribution on the contact areas (see Figure 1).

To model the geometry, it is simple to use a regular mesh, which is straightforward to generate. However, this would require a very long computer time for a given accuracy. The preferred strategy is to use a fine meshing in deformed regions and a coarse mesh in regions that are less deformed. The mesh density is selected according to the experience gained with finite element calculation of the PCCv specimen loaded in three point bending [11]. The mesh contains 5120 elements and 6184 nodes and is depicted in Figure 2.
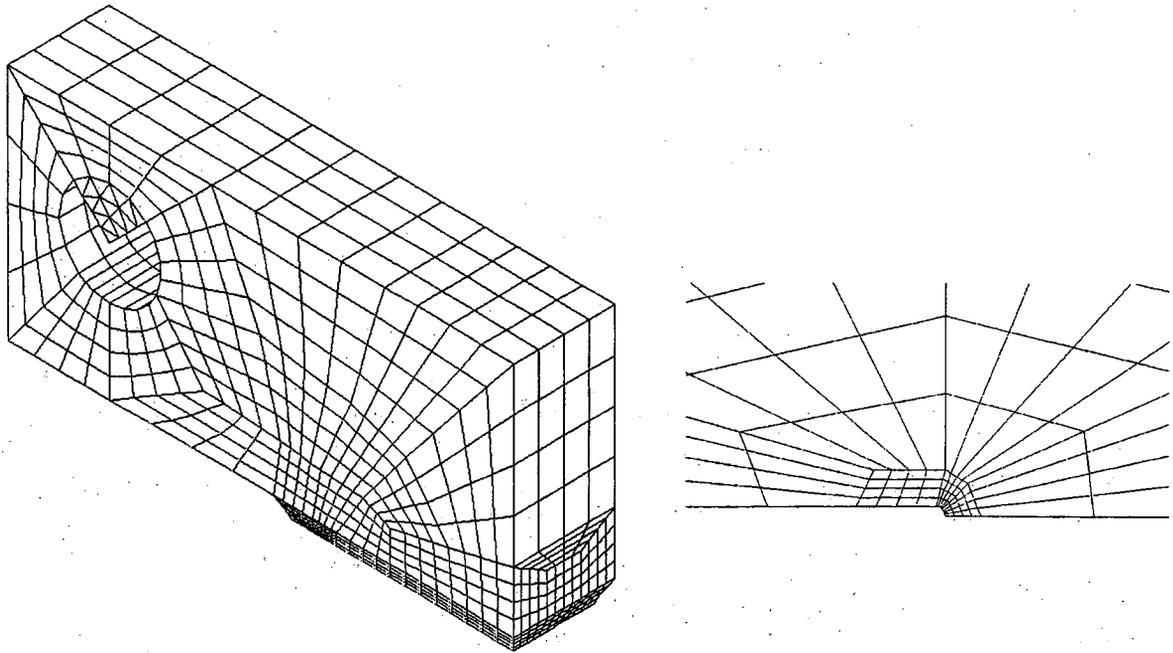
Figure 2 *Meshing of a 1T C(T) specimen with side-grooves.*

The finite element code used, SYSWORLD, is a standard commercial code developed by the ESI group [13]. The algorithm used for the matrix inversion uses an iterative method to decrease the size of the required RAM memory. The resolution of non-linear equations is performed using the BFGS algorithm. The number of load increments is typically 50.

The machine used for this project is a SUN Ultra 1 model 170E equipped with a Creator 3D graphic card. This machine has a single processor, which operates at 167 MHz. The RAM is 1024 MB. The machine is equipped with two disks of 18.1 GB. The central process unit (CPU) time per load increment is 832 sec. The complete resolution takes more time as the CPU time is always lower than the elapsed time and the pre- and post-processing time is not included.

3 Finite element results

The load versus crack mouth opening displacement (CMOD) is given in Figure 3. The initial crack mouth opening or gauge length is taken equal to 2.74 mm. The CMOD is equivalent to the load line displacement (LLD) for a C(T) specimen. Figure 3 shows that a quasi linear behaviour is observed up to a K level of 100 MPa$\sqrt{m}$.
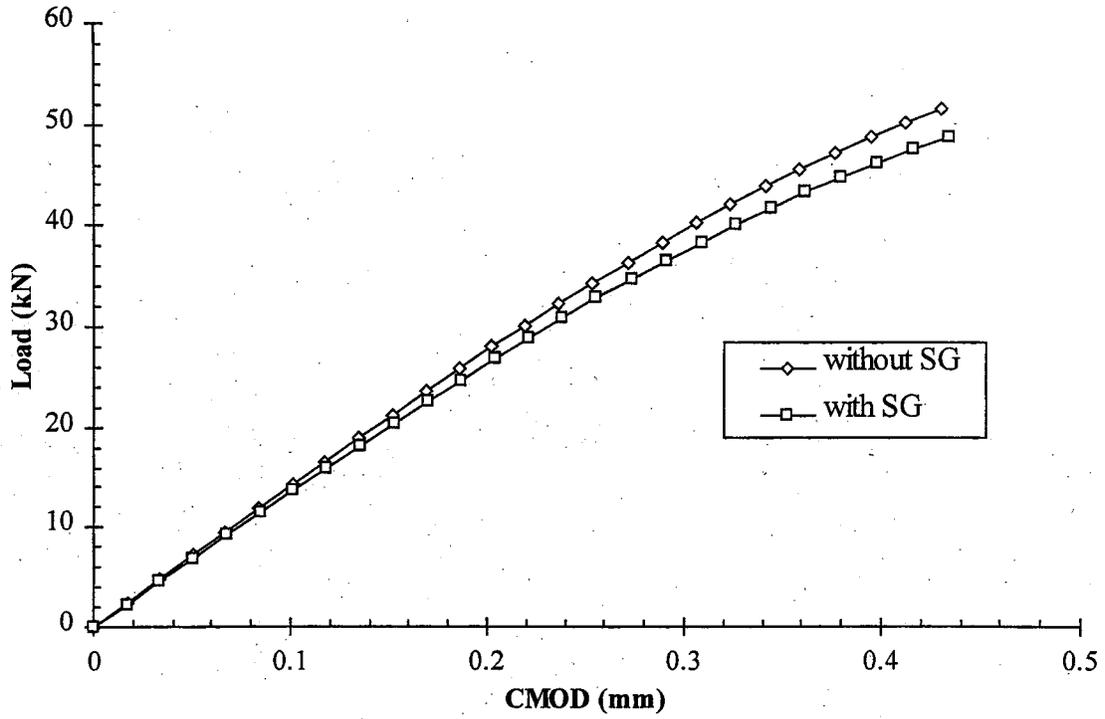
Figure 3 *Load versus CMOD (LLD) for a 1T C(T) specimen.*

For C(T) specimens, ASTM E1921-97 gives a formula to evaluate the fracture toughness from the load versus displacement record. This method is now assessed and compared to the direct evaluation of the J-integral.

The J-integral for a C(T) specimen is evaluated as [1]:

$$J = \frac{K_e^2}{E} + J_p \tag{6}$$

where:

$$K_e = \frac{P}{(BB_N W)^{1/2}} f(a_0 / W) \tag{7}$$

$$f(a_0 / W) = \frac{\left[\begin{array}{l}(2 + a_0 / W)(0.886 + 4.64(a_0 / W) \\ -13.32(a_0 / W)^2 + 14.72(a_0 / W)^3 - 5.6(a_0 / W)^4)\end{array}\right]}{(1 - a_0 / W)^{3/2}} \tag{8}$$

where P is the load, a_0 the initial crack length, W the specimen width, B the specimen thickness and B_N the specimen net thickness.

The standard method to evaluate the plastic component of the J-integral, J_p, is based on the measure of the load line displacement, which is measured using a clip gauge located on the load line. The standard proposes:

$$J_p = \frac{\eta A_p}{B_N b_0} \qquad \text{with} \qquad \eta=2+0.522\ b_0/w \qquad (9)$$

where b_0 is the initial ligament length ($b_0=W-a_0$).

A_p is the plastic area under the load (P) versus load-line displacement curve given by:

$$A_p=A-1/2C_0P \qquad (10)$$

where A is the total area under the load versus load-line displacement curve and C_0 the reciprocal of the initial elastic slope.

The standard methodology to evaluate the J-integral can be compared to a direct evaluation of the J-integral from the finite element calculations. For a 3-D configuration, the loading of the specimen is measured through the average J-integral along the crack front, which is defined as:

$$J = \frac{1}{L}\lim_{\varepsilon \to 0} \int_{A_\varepsilon} (Wn_x - \sigma_{ij}\partial_x u_i n_j)dA_\varepsilon \qquad (11)$$

where x is the direction of crack propagation, L the crack length, A_ε a tubular surface around the crack front, W the energy density, n the external normal to A_ε, σ the stress tensor and u the displacement vector.

The J-integral as expressed in equation (11) cannot be directly and accurately evaluated from the finite element results, as just ahead of the crack tip large stresses and strain gradients are expected. Therefore, the J-integral is transformed into an equivalent domain integral (EDI) [12, 14]. In the absence of thermal load, volumic forces and stresses or displacements applied to the crack lips, the EDI reduces to:

$$J = \frac{-1}{L}\int_V (W\partial_x q - \sigma_{ij}\partial_x u_i \partial_j q)dV \qquad (12)$$

where V is a tubular volume around the crack front, q any continuous function with a value of one at the crack tip and zero at the external border of V. In this work, q is chosen equal to a quadratic function of the radial coordinate with a slope of zero at the crack tip front and at the external border of V [15].

From a theoretical point of view, the J-integral obtained from the EDI method is independent from the size of the tubular volume under different hypotheses [15]: small strain, proportional loading with no partial unloading and existence of a potential function with a unique relationship between stress and strain.

The J-integral will be evaluated with the EDI method using a cylindrical volume with the largest radius (the radius is 25 mm for a C(T) with a/W=0.5). The effect of the radius size was already investigated in [11].

Taking the J-integral calculated by the EDI method as the reference value, the ASTM E1921-97 standard method is compared in Figure 4. It shows that the standard methods have an

acceptable accuracy of 3% on K_J. This 3% error on K_J causes an error of 1 °C only on the reference temperature, T_0.
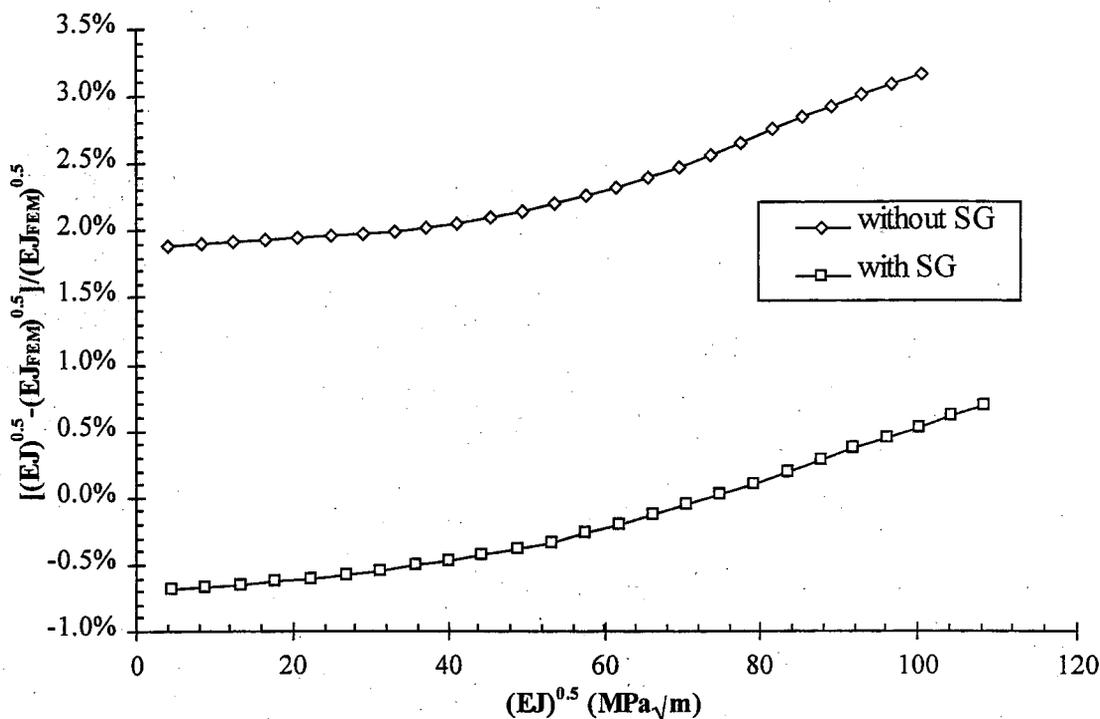

Figure 4 *Comparison of J obtained from the load versus load-line displacement curves with the J-integral calculated from finite element calculations.*

The constraint of the PCCv specimen is now compared to the constraint of a 1T C(T) specimen. When no loss of constraint correction is taken into account, the reference temperature for a PCCv specimen is obtained as:

$$T_{0,PCCv} = T - \frac{1}{0.019} \ln\left(\frac{K_{med,1T} - 30}{70} \right)$$ (13)

where T is the test temperature, $K_{med,1T}$ is the median fracture scaled to one inch:

$$K_{med,1T} = 20 + (K_{med} - 20)\left(\frac{B}{B_{1T}} \right)^{1/4}$$ (14)

where K_{med} is the median fracture toughness of the PCCv specimens, B the original specimen thickness (according to the standard the net thickness B_N should not be used) and B_{1T} a reference length of one inch.

To take loss of constraint into account a simple model proposed by Anderson and Dodds [16] and developed in [12] is used. The reference temperature is obtained using:

$$T_{0,C(T)} = T - \frac{1}{0.019} \ln\left(\frac{K_{med,1T,C(T)} - 30}{70} \right)$$ (15)

where $K_{med,1T,C(T)}$ is the median fracture of the PCCv specimens corrected for loss of constraint to an equivalent 1T C(T) specimen:

$$K_{med,1T,C(T)} = 20 + (K_{med} - 20)\left(\frac{A_{PCCv}}{A_{C(T)}} \frac{B}{B_{1T}}\right)^{1/4} \qquad (16)$$

with

$$A = \frac{\sigma_{YS}^2 \varepsilon_{YS}^2}{B\,J^2} V(\sigma_1) \qquad (17)$$

where $V(\sigma_1)$ is the volume over which the maximum principal stress is equal or greater than a certain value σ_1.

The dimensionless area, A, is given in Figure 5 as a function of the principal stress. This dimensionless area is obtained by finite element calculations on four different configurations, SSY plane stress, SSY plane stress, PCCv and C(T). SSY refers to the Small Scale Yielding solution, which is a 2D solution of a small plastic zone embedded in a large elastic zone [12].
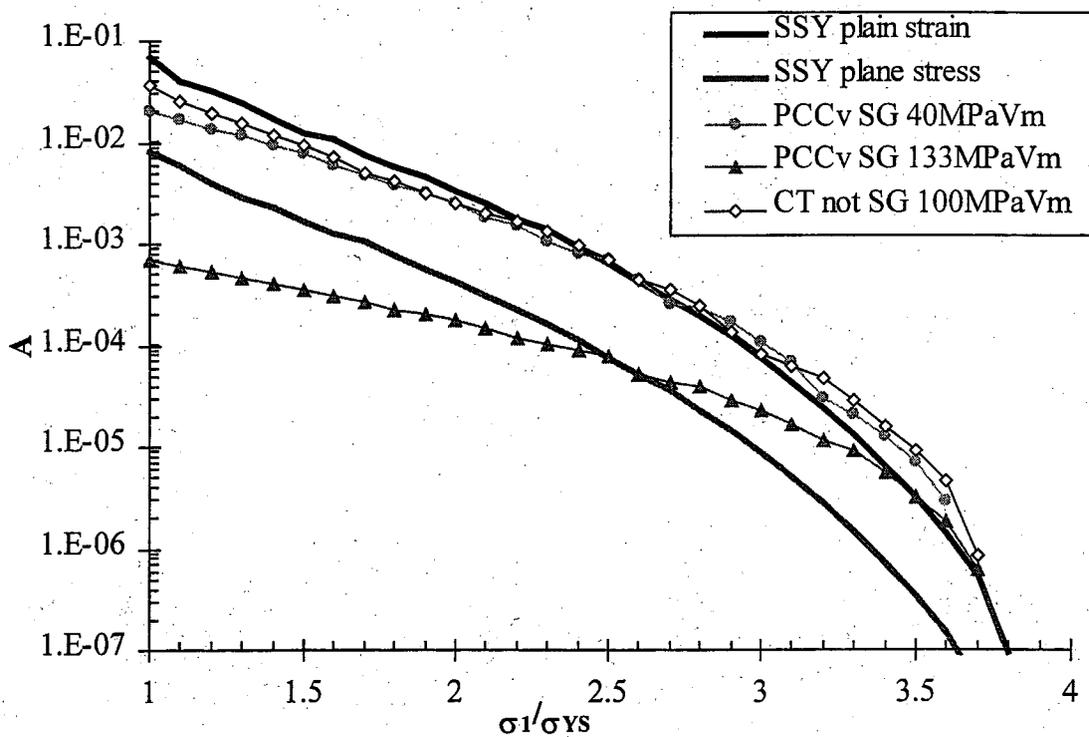

Figure 5 Dimensionless area, A, for which the maximum principal stress is above a given value σ_l.

It is now possible to evaluate the loss of constraint through:

$$\Delta T = T_{0,PCCv} - T_{0,C(T)} \qquad (18)$$

ΔT is given in Figure 6 as a function of K_{med} and σ_1. The geometry studied is the 20 % side grooved PCCv and the reference solution is the non-side grooved on 1T C(T) geometry.
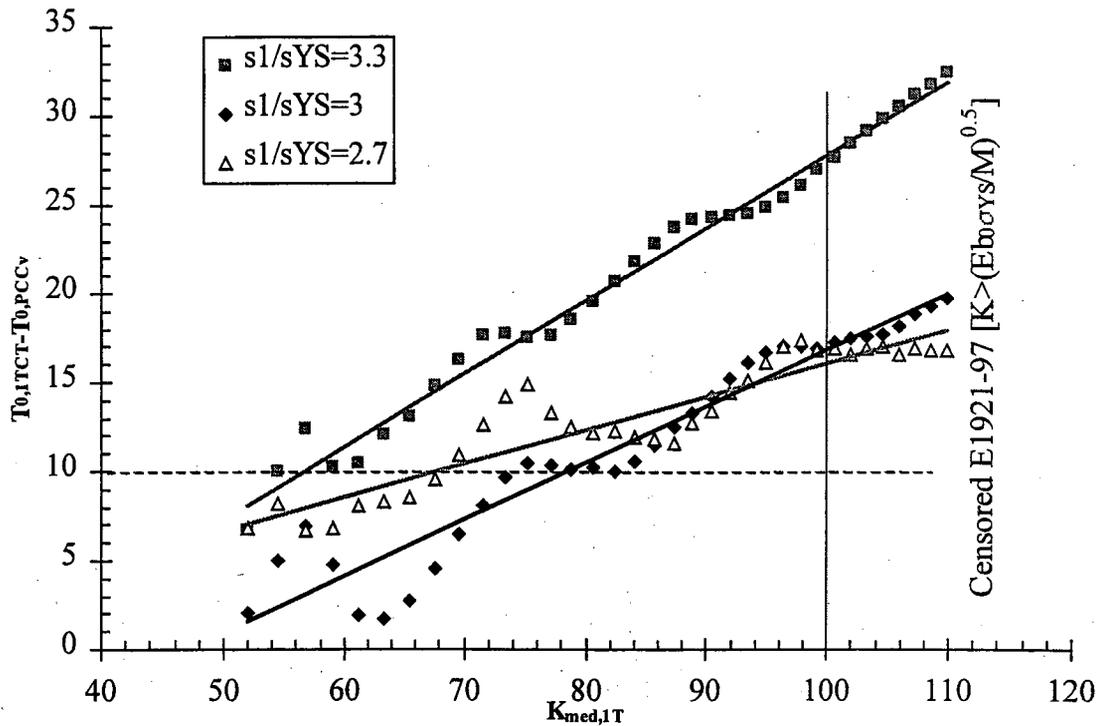

Figure 6 *Loss of constraint in terms of reference temperature as a function of the median fracture toughness normalised to 1T and for different critical stresses.*

4 Discussion

The parameters used to calculate the J-integral obtained in the present investigation are compared to the ASTM E1921-97 standard in Table 1. In accordance with [10], η is obtained by the slope of the linear fit imposing that the intercept be equal to 0 as illustrated in Figure 7.

This difference was found to be as small as 10% on the J-integral and corresponds to 5% on K_J and to 3 °C in terms of reference temperature T_0. The η-factor evaluated in Figure 7, should not be considered to be applicable to the whole range of a C(T) specimen as in the present study the J-integral is predominantly governed by the elastic part. Calculations up to the limit of validity could lead to slightly different results in term of η-factor.

			this work	[10]	ASTM E1921-97
	f(a/W)	not SG	9.94	n.a.	9.66
a/W=0.5		SG 20%	10.20	n.a.	9.66
	η	not SG	2.029	n.a.	2.261
		SG 20%	1.917	n.a.	2.261
a/W=0.6	η	not SG	n.a.	2.17	2.209
		SG 20%	n.a.	2.08	2.209

Table 1 *Comparison of the parameters used to calculate the stress intensity factor K and the J-integral. Calculations are done for a C(T) specimen with n=0.1 and $E/\sigma_{YS}=500$.*
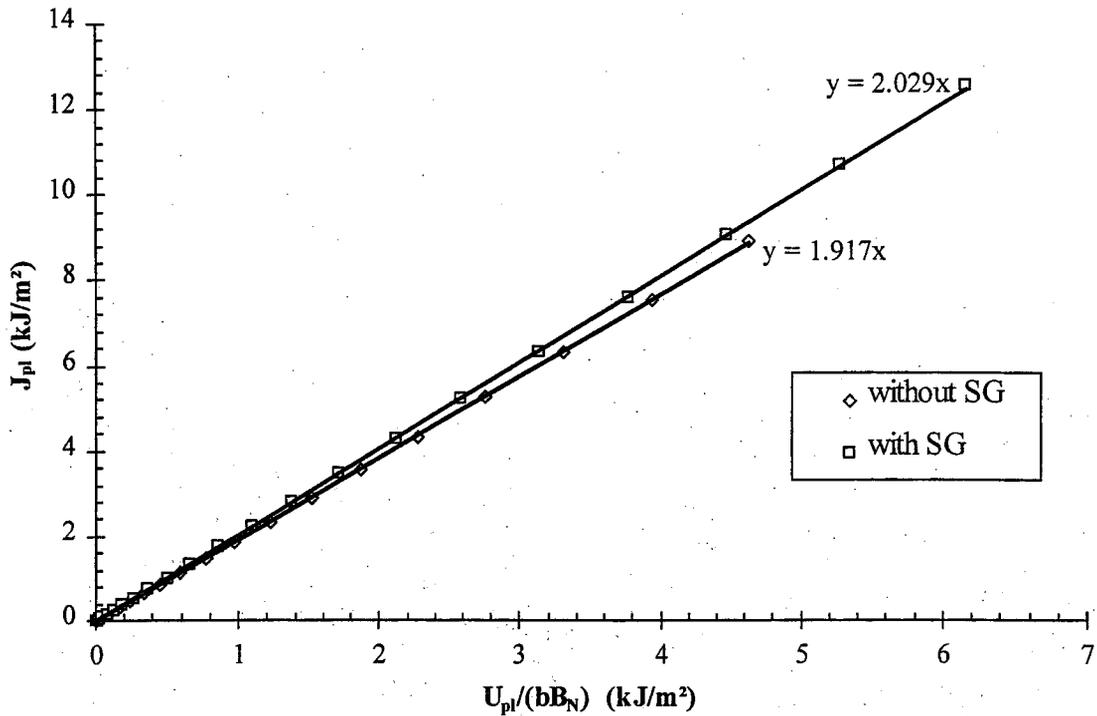
Figure 7 η *is obtained from the slope of the linear fit imposing the intercept equal to 0.*

The constraint of a bend geometry can be discussed based on Figure 5. Up to 40 MPa√m, no constraint difference is observed between 1T C(T) and PCCv. It is clear that at a relatively low load, 1T C(T) and PCCv specimens are closer to plane strain than plane stress. The constraint just ahead of the crack tip at $\sigma_1/\sigma_{YS}=3.5$ is even higher than the plane stress SSY solution. Two explanations are possible:

- In [7], the T-stress is calculated in both geometries. The T-stress is a hydrostatic stress obtained from an elastic calculation, which is added to the plane stress SSY solution. The T-stress is normalised using the geometry ratio [7], β:

$$T=\beta K/(\pi a)^{0.5} \tag{19}$$

It is found that C(T) and SE(B) specimens have a positive geometry ratio, β, of respectively 0.6 and 0.2. This means that than the SSY plane strain, which is the reference solution, has a lower constraint than C(T) and SE(B) specimens.

- The mesh size was verified to be fine enough to obtain a global convergence, which means that the load versus displacement curve is independent of the mesh size. Figure 5 was also calculated using a more refined mesh for the C(T) configuration containing 10000 elements and 11688 nodes. It is found that it has practically no effect on the dimensionless area versus principal maximal stress curve. However, as can be seen in Figure 8, the mesh size is still too rough and the transition between small and larger element is not smooth enough to correctly represent stress just ahead of the crack tip. Our current computation capabilities do not allow us to use much more refined mesh. Therefore, it is still possible that this higher constraint level is only an artefact due to insufficient mesh refinement.
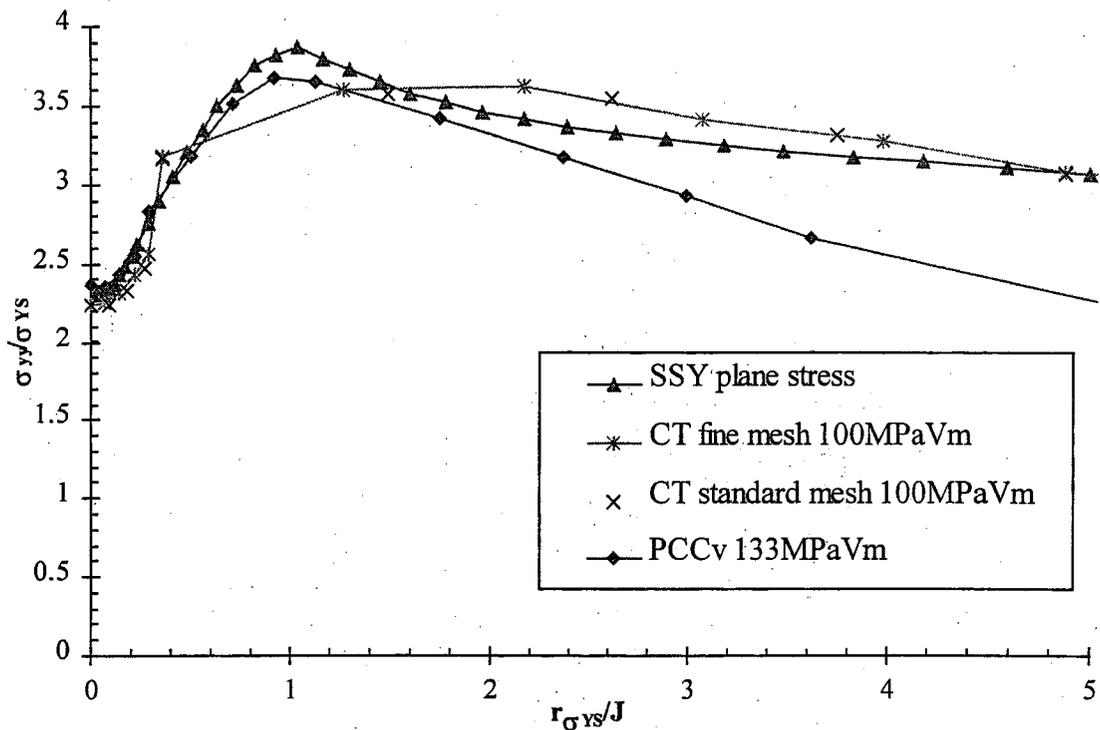
Figure 8 *Maximum principal stress ahead of the crack tip along the line of intersection between the two symmetry planes.*

Figure 5 clearly shows a loss of constraint with loading level for the PCCv geometry. This loss of constraint is strongly dependent on the maximum principal stress considered or equivalently to the considered distance. Consequently, the scaling results, illustrated in Figure 6, depend on the maximum principal stress level considered. This means that a better description of the failure mechanism such as the BEREMIN model [18], would be required to further determine the effect of loss of constraint. In a recent work, Ruggieri et al. [19] demonstrated the non-uniqueness of the (m, σ_u) parameters of the BEREMIN model. They found a strong sensitivity of corrected J_c-value on parameter m. This means that the constraint correction is a function of the failure mechanism. It should be noted that for the CRB geometry, the loss of constraint correction was found to be nearly independent of the maximum stress considered [12]. Taking a plausible stress contour of 2.7 to 3.3 times σ_{YS}, it is found that PCCv specimens tested at the same temperature than 1T C(T) specimens should lead to about 10 °C lower reference temperatures. This does not mean that SE(B) specimens lead to lower reference temperature than C(T) specimens. This issue could be investigated by performing calculation on SE(B) and C(T) specimens having the same ligament size. Indeed, the ligament size of a PCCv specimen is 5 times smaller than a 1T C(T) specimen.

CONCLUSIONS AND RECOMMENDATIONS

Three-dimensional finite element calculations were performed on side-grooved and non side-grooved PCCv and C(T) specimens for a/W=0.5. The fracture toughness determination and loss of constraint assessment were addressed in this report.

The main deliverables of this investigation are:

- Although it can be improved, the formulation proposed in the ASTM E1921-97 to calculate the J-integral for a 1T C(T) is sufficiently accurate for its application. The maximum error on the reference temperature is 3 °C.
- C(T) and PCCv specimens display a plane strain behaviour at low load levels.
- Up to 40 MPa√m no constraint difference between PCCv and 1T C(T) is observed.
- C(T) and PCCv specimens are possibly more constrained geometries than the SSY plane strain condition.
- For a PCCv loaded above 40 MPa√m, which correspond to $M_{PCCv}=270$, the constraint decrease as compared with 1T C(T).
- The model used predicts a reference temperature about 10 °C lower for a PCCv specimen as compared to a 1T C(T) specimen. This is an important result that is supported by a large experimental database.

The following additional research work is recommended:

- To study the possible difference of constraint between SE(B) and C(T), additional calculations on specimen having the same ligament size would be required.
- To study the transition between plane strain versus plain stress condition, it would be interesting to determine characteristic quantities such as $A_{PCCv}(z)$, $J(z)$, $\varepsilon_z(z)$ along the crack front. However, it is not straightforward to extract and process finite element results to obtain these quantities.
- An improved mesh design in conjunction with improved computation capabilities would allow to better describe the stress field just ahead of the crack tip.
- The application of constraint correction for data set that contains few or any valid data would also requires additional work in order to extend the range investigated here and to apply the model developed in [19].

ACKNOWLEDGEMENTS

REFERENCES

[1] ASTM E 1921-97 "Test method for the determination of reference temperature, T_0, for ferritic steels in the transition range", Annual book of ASTM standards, Section 3, Vol. 03.01 Metals Test Methods and Analytical Procedures, Printed in Easton, MD, USA, 2000

[2] E. van Walle "Reconstitution: where do we stand ?", Effects of irradiation on materials: 17th international symposium, ASTM STP 1270, D.S. Gelles, R.K. Nansdstad, A.S. Kumar and E.A. Little, Eds., American Society for Testing Materials, 415-441, 1996

[3] K. Wallin "Applicability of miniature size bend specimens to determine the master curve T_0 Temperature", IGRDM-9, Leuven, Belgium, September 2000

[4] E. Lucon and M. Scibetta "Comparison between precracked Charpy-V and C(T) specimens for T_0 determination of the JSPS RPV steel", report R-3378 Rev. 1, SCK•CEN, Mol, Belgium, January 2000

[5] R. Chaouadi, M. Scibetta, E. van Walle and R. Gerard "On the use of the master curve based on the precracked charpy specimen", Pressure Vessel and Piping Symposium, "Fracture, Fatigue and Weld Residual Stress ", Vol 393, pp. 35 -46, 1999

[6] Lee Bong-Sang, Yang Won-Jon, Kim Joo-Hag, Hong Jun-Hwa and Lee Byong-Whi "Determination of the fracture toughness transition temperature, T_0, of the IAEA and Korean Reference Materials, JRQ, JFL, KFY5", presented at the RCM of the CRP on "Assuring Structural Integrity of Reactor Pressure Vessels", Vienna Austria, November 17-19, 1999

[7] Tregoning, R.L. and Joyce, J.A., "T_0 Evaluation in Common Specimen Geometries," ASME PVP Vol. 412, Applications of Fracture Mechanics in Failure Assessment, Lidbury, D., Ed., ASME, 2000, pp. 143-152.

[8] Joyce, J.A. and Tregoning, R.L., "Development of the T_0 Reference Temperature From Precracked Charpy Specimens", ASME PVP Vol. 393, Fracture, Fatigue and Weld Residual Stress, Pan, J., Ed., ASME, 1999, pp. 53-62.

[9] Dodds R.H., Carpenter W.C. and Sorem W.A. "Numerical evaluation of a 3-D J-integral and comparison with experimental results for a 3-point bend specimen", Engineering Fracture Mechanics Vol. 29, No. 3, pp. 275-285, 1988

[10] Nevalainen M. and Dodds R.H.Jr. "Numerical investigation of 3-D Constraint Effects on Brittle Fracture in SE(B) and C(T) Specimens", Report UILU-ENG-95-2001, Department of civil engineering, university of illinois at Urbana-Champaign Urbana, Illinois, February 1995

[11] M. Scibetta "3-D Finite Element Simulation of the PCCv Specimen Statically Loaded in Three-Point Bending" Convention Electrabel-SCK•CEN, Report R-3440, SCK•CEN, Mol, Belgium, 2000

[12] Scibetta M. "Contribution to the Evaluation of the Circumferentially-Cracked Round Bar for Fracture Toughness Determination of Reactor Pressure Vessel Steels", Dissertation for the Degree of Doctor in Applied Sciences, Université de Liège, March 1999.

[13] ESI Group, SYSTUS+ 2.0, Analysis Reference Manual, 1998

[14] Nikishkov G.P. and Alturi S.N. "Calculation of fracture mechanics parameters for an arbitrary three-dimensional crack, by the 'equivalent domain integral' method", Int. Journal for numerical methods in engineering, Vol. 24, pp. 1801-1821, 1987

[15] Scibetta M. "Fracture toughness evaluation of circumferentially-cracked round bars", report BLG-716, SCK-CEN Mol, Belgium, May 1996

[16] Anderson T.L. and Dodds R.H. Jr. "Simple constraint corrections for subsize fracture toughness specimens", Small Specimen Test Techniques Applied to Nuclear Reactor Vessel Thermal Annealing and Plant Life Extension, ASTM STP 1204, Corwin W.R., Haggag F.M. and Server W.L., Eds., American Society for Testing and Materials, Philadelphia, pp. 93-105, 1993

[17] Koppenhoefer K. C. and Dodds R.H. "Loading rate effects on cleavage fracture of pre-cracked CVN specimens: 3-D studies", Engineering Fracture Mechanics Vol. 58, No. 3, pp. 249-270, 1997

[18] Beremin F.M. "A local criterion for cleavage fracture of a nuclear pressure vessel steel", Metallical transactions A, Vol. 14A, pp. 2277-2287, 1987

[19] Ruggieri C., Gao X., Dodds R.H.Jr. "Transferability of the elastic-plastic fracture toughness using the Weibull stress approach: significance of parameter calibration", Engineering Fracture Mechanics 67, pp. 101-117, 2000